

Complementary response of static spin-stripe order and superconductivity to non-magnetic impurities in cuprates

Z. Guguchia,^{1,2,*} B. Roessli,³ R. Khasanov,¹ A. Amato,¹ E. Pomjakushina,⁴
K. Conder,⁴ Y.J. Uemura,² J.M. Tranquada,⁵ H. Keller,⁶ and A. Shengelaya^{7,8}

¹Laboratory for Muon Spin Spectroscopy, Paul Scherrer Institute, CH-5232 Villigen PSI, Switzerland

²Department of Physics, Columbia University, New York, NY 10027, USA

³Laboratory for Neutron Scattering and Imaging,

Paul Scherrer Institut, CH-5232 Villigen, Switzerland

⁴Laboratory for Developments and Methods, Paul Scherrer Institut, CH-5232 Villigen PSI, Switzerland

⁵Condensed Matter Physics and Materials Science Division,
Brookhaven National Laboratory, Upton, NY 11973, USA

⁶Physik-Institut der Universität Zürich, Winterthurerstrasse 190, CH-8057 Zürich, Switzerland

⁷Department of Physics, Tbilisi State University, Chavchavadze 3, GE-0128 Tbilisi, Georgia

⁸Andronikashvili Institute of Physics of I.Javakhishvili Tbilisi State University, Tamarashvili str. 6, 0177 Tbilisi, Georgia

We report muon-spin rotation and neutron-scattering experiments on non-magnetic Zn impurity effects on the static spin-stripe order and superconductivity of the La214 cuprates. Remarkably, it was found that, for samples with hole doping $x \approx 1/8$, the spin-stripe ordering temperature T_{so} decreases linearly with Zn doping y and disappears at $y \approx 4\%$, demonstrating a high sensitivity of static spin-stripe order to impurities within a CuO_2 plane. Moreover, T_{so} is suppressed by Zn in the same manner as is the superconducting transition temperature T_c for samples near optimal hole doping. This surprisingly similar sensitivity suggests that the spin-stripe order is dependent on intertwining with superconducting correlations.

PACS numbers: 74.72.-h, 74.62.Fj, 75.30.Fv, 76.75.+i

One of the most astonishing manifestations of the competing ordered phases occurs in the system $\text{La}_{2-x}\text{Ba}_x\text{CuO}_4$ (LBCO) [1], where the bulk superconducting (SC) transition temperature T_c exhibits a deep minimum at $x = 1/8$ [2–4]. At this doping level muon-spin rotation (μSR), neutron, and x-ray diffraction experiments revealed two-dimensional static charge and spin-stripe order [5–11]. The collected experimental data indicate that the tendency toward uni-directional stripe-like ordering is common to cuprates [3, 4, 12–14]. However, the relevance of stripe correlations for high-temperature superconductivity remains a subject of controversy. On the theoretical front, the concept of a sinusoidally-modulated pair-density wave (PDW) SC order, intimately intertwined with spatially modulated antiferromagnetism, has been introduced [15–17]. On the experimental front, quasi-two-dimensional superconducting correlations were observed in $\text{La}_{1.875}\text{Ba}_{0.125}\text{CuO}_4$ (LBCO-1/8) and $\text{La}_{1.48}\text{Nd}_{0.4}\text{Sr}_{0.12}\text{CuO}_4$, coexisting with the ordering of static spin-stripes, but with frustrated phase order between the layers [18–23]. Recently, it was found that in $\text{La}_{2-x}\text{Ba}_x\text{CuO}_4$ ($0.11 \leq x \leq 0.17$) the 2D SC transition temperature T_{c1} and the static spin-stripe order temperature T_{so} have very similar values throughout the phase diagram [24, 25]. Moreover, a similar pressure evolution of T_c and T_{so} in the stripe phase of $x = 0.155$ and 0.17 samples was observed. These findings were discussed in terms of a spatially modulated and intertwined pair wave function [15–17, 26]. There are also a few reports proposing the relevance of a PDW state in sufficiently underdoped $\text{La}_{2-x}\text{Sr}_x\text{CuO}_4$ [27] and

$\text{YBa}_2\text{Cu}_3\text{O}_{6-x}$ [28, 29]. At present it is still unclear to what extent PDW order is a common feature of cuprate systems where stripe order occurs.

To further explore the interplay between static stripe order and superconductivity in cuprates we used non-magnetic impurity substitution at the Cu site as an alternative way of tuning the physical properties. Since the discovery of cuprate HTSs much effort was invested in the investigation of the effect of in-plane impurities. It is now well established that in cuprate HTSs nonmagnetic Zn ions suppress T_c even more strongly than magnetic ions [30–32]. Such behaviour is in sharp contrast to that of conventional superconductors. This observation led to

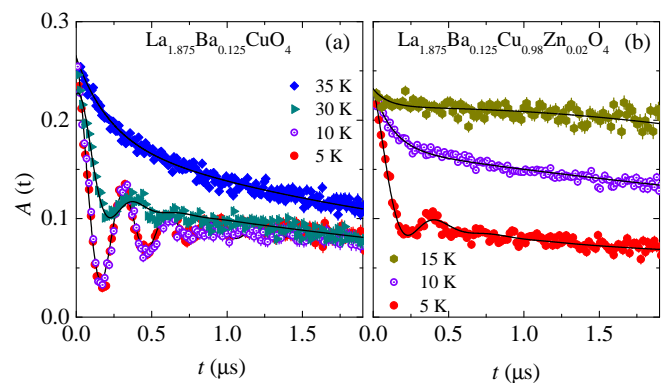


FIG. 1: (Color online) Zero-field (ZF) μSR time spectra $A(t)$ for $\text{La}_{1.875}\text{Ba}_{0.125}\text{CuO}_4$ (a) and $\text{La}_{1.875}\text{Ba}_{0.125}\text{Cu}_{0.98}\text{Zn}_{0.02}\text{O}_4$ (b) recorded at various temperatures. The solid lines represent fits to the data by means of Eq. (3) of methods section.

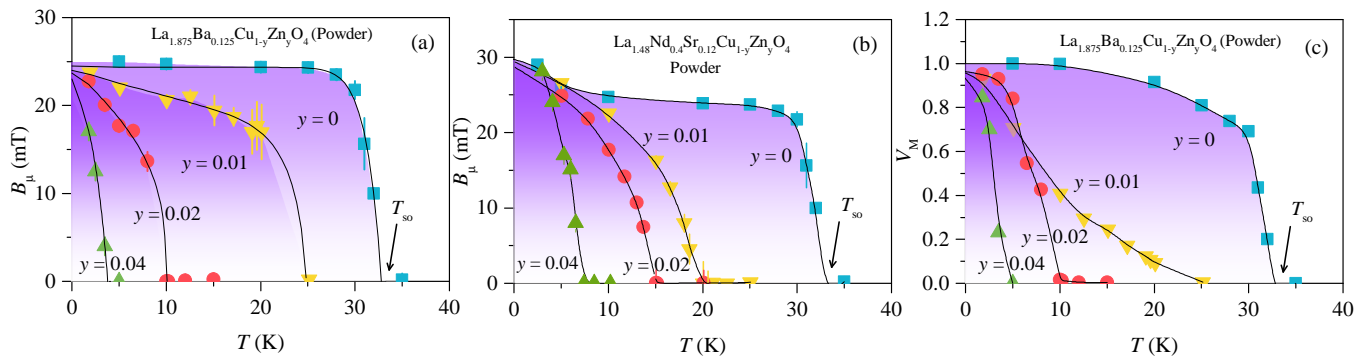


FIG. 2: (Color online) The temperature dependence of the internal magnetic field B_μ (a) and the magnetic fraction V_M (c) for the polycrystalline samples of $\text{La}_{1.875}\text{Ba}_{0.125}\text{Cu}_{1-y}\text{Zn}_y\text{O}_4$ ($y = 0, 0.02, 0.04$). The temperature dependence of B_μ for the polycrystalline samples of $\text{La}_{1.48}\text{Nd}_{0.4}\text{Sr}_{0.12}\text{Cu}_{1-y}\text{Zn}_y\text{O}_4$ ($y = 0, 0.01, 0.02, 0.04$) (b). The arrows mark the spin-stripe order temperature T_{so} . The solid curves are fits of the data to the power law $B_\mu(T) = B_\mu(0)[1-(T/T_{so})^\gamma]^\delta$, where $B_\mu(0)$ is the zero-temperature value of B_μ . γ and δ are phenomenological exponents.

the formulation of an unconventional pairing mechanism and symmetry of the order parameter for cuprate HTSs. In addition, in several cases a ground state with static antiferromagnetic (AF) correlations is stabilized by Zn-doping [33–38]. Up to now much less is known concerning impurity effects on the static stripe phase in cuprates at 1/8 doping. From specific heat and neutron scattering measurements it was inferred that Zn doping leads to stripe destruction [3, 39, 41]. Such an effect is very interesting and it was not predicted theoretically. However, no systematic impurity effect studies on static stripe order have been carried out up to now. Moreover, specific heat is a very indirect method to characterize the stripe phase in cuprates. Therefore, it is very important to use experimental techniques which can directly probe stripe formation and its evolution with impurity doping.

In this letter, we report on systematic muon-spin rotation μSR , neutron scattering, and magnetization studies of Zn impurity effects on the static spin-stripe order and superconductivity in the La214 cuprates. Remarkably, it was found that in these systems the spin-stripe ordering temperature T_{so} decreases linearly with Zn doping y and disappears at $y \approx 4\%$. This means that T_{so} is suppressed in the same manner as the superconducting transition temperature T_c by Zn impurities. These results suggest that the stripe and SC orders may have a common physical mechanism and are intertwined.

In a μSR experiment, positive muons implanted into a sample serve as an extremely sensitive local probe to detect small internal magnetic fields and ordered magnetic volume fractions in the bulk of magnetic systems. Thus μSR is a particularly powerful tool to study inhomogeneous magnetism in materials [42]. Neutron diffraction experiments [43] allow to directly probe the incommensurate spin structure of spin-stripe order and thus provide crucial complementary information to the μSR technique.

Figures 1(a) and (b) show representative zero-field (ZF) μSR time spectra for polycrystalline

$\text{La}_{1.875}\text{Ba}_{0.125}\text{Cu}_{1-y}\text{Zn}_y\text{O}_4$ samples with $y = 0$ and 0.02, respectively, recorded at various temperatures. For $y = 0$, damped oscillations due to muon-spin precession in internal magnetic fields are observed below $T_{so} \approx 35$ K, indicating the formation of static spin order in the stripe phase [1, 2, 4, 9, 25, 45]. It is seen in Fig. 1(b), that for the $y = 0.02$ sample the oscillating signal appears only below $T \approx 10$ K, showing strong suppression of the static spin-stripe order with Zn doping. We have studied this novel effect systematically as a function of Zn doping.

The temperature dependence of the average internal field B_μ , which is proportional to the ordered magnetic moment, is shown in Fig. 2(a) for various Zn dopings y . As evident from Fig. 2(a), $B_\mu(0)$, the internal magnetic field extrapolated to zero-temperature, does not de-

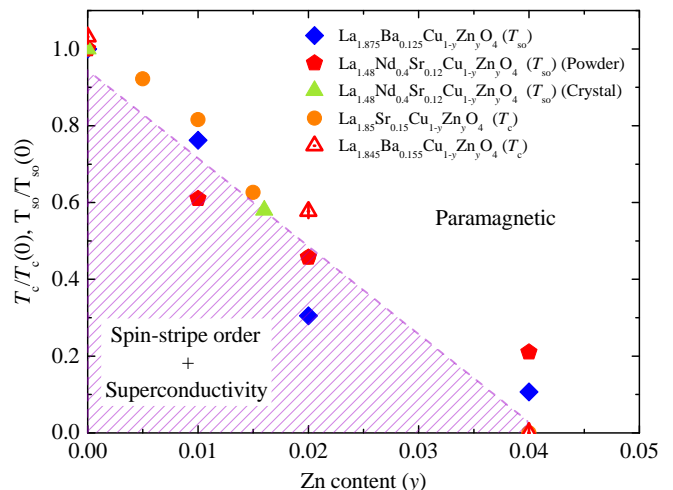


FIG. 3: (Color online) The normalised static spin-stripe order temperature $T_{so}/T_{so}(0)$ for $\text{La}_{1.875}\text{Ba}_{0.125}\text{Cu}_{1-y}\text{Zn}_y\text{O}_4$ and $\text{La}_{1.48}\text{Nd}_{0.4}\text{Sr}_{0.12}\text{Cu}_{1-y}\text{Zn}_y\text{O}_4$ as a function of Zn content y . The superconducting transition temperature $T_c/T_c(0)$ of $\text{La}_{1.85}\text{Sr}_{0.15}\text{Cu}_{1-y}\text{Zn}_y\text{O}_4$ as a function of Zn content y . The dashed line is a guide to the eye.

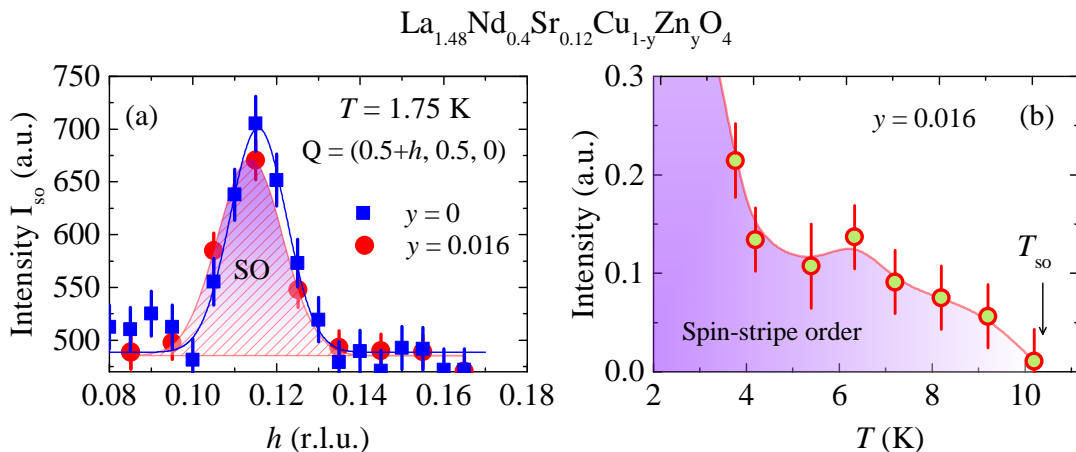


FIG. 4: (Color online) (a) h -scans through the SO-peak at $(0.5+h, 0.5, 0)$ for the single crystals of $\text{La}_{1.48}\text{Nd}_{0.4}\text{Sr}_{0.12}\text{Cu}_{1-y}\text{Zn}_y\text{O}_4$ ($y = 0, 0.016$), recorded at the base temperature $T = 1.75$ K. The intensities have been normalized to the crystal volume in the neutron beam. The solid lines represent the Gaussian fits to the data. (b) Peak intensity versus temperature of the $(0.5+h, 0.5, 0)$ SO-peak, normalized to the crystal volume in the neutron beam.

pend on the Zn content y , while T_{so} changes substantially with increasing y . Specifically, T_{so} decreases from $T_{\text{so}} \simeq 32.5$ K for $y = 0$ to $T_{\text{so}} \simeq 4$ K for $y = 0.04$. Figure 2(b) shows that a very similar behavior is observed for B_μ measured on polycrystalline samples of the related compound $\text{La}_{1.48}\text{Nd}_{0.4}\text{Sr}_{0.12}\text{Cu}_{1-y}\text{Zn}_y\text{O}_4$. Note that the low-temperature value of B_μ is enhanced by the ordering of the Nd moments. A similar suppression of T_{so} by Zn impurities was also observed in single-crystal samples of $\text{La}_{1.48}\text{Nd}_{0.4}\text{Sr}_{0.12}\text{Cu}_{1-y}\text{Zn}_y\text{O}_4$ ($y = 0, 0.016$). It seems that this effect is a generic feature of cuprates with static stripe order. We note that in all the above mentioned systems, despite the suppression of T_{so} with Zn doping, the magnetic volume fraction V_m at the base temperature stays nearly 100% [see Fig. 2(c)]. The bulk LTT structural phase transition temperature also stays nearly unaffected by Zn-doping (see supplementary Note II and supplementary Fig. S1 [42]).

The observed Zn impurity effects on T_{so} in $\text{La}_{1.875}\text{Ba}_{0.125}\text{Cu}_{1-y}\text{Zn}_y\text{O}_4$ and $\text{La}_{1.48}\text{Nd}_{0.4}\text{Sr}_{0.12}\text{Cu}_{1-y}\text{Zn}_y\text{O}_4$ are summarised in Fig. 3. It is a remarkable finding that T_{so} linearly decreases with increasing Zn content y . Such a behaviour is reminiscent of the well known linear suppression of the SC transition temperature T_c in cuprates [30–32]. Since the superconducting volume fraction in 1/8 doped samples is tiny and the bulk T_c is also very low, it is difficult to follow the SC properties of these systems as a function of Zn content. Alternatively, in Fig. 3 we plot T_c values for optimally doped $\text{La}_{1.85}\text{Sr}_{0.15}\text{CuO}_4$ [30–32] and $\text{La}_{1.845}\text{Ba}_{0.155}\text{CuO}_4$ (see below) as a function of Zn content. Strikingly, suppression of T_{so} goes in a very similar manner as the well known impurity-induced T_c suppression.

We have confirmed the Zn doping effect on the static spin-stripe order by neutron diffraction experiments on

single-crystal samples of $\text{La}_{1.48}\text{Nd}_{0.4}\text{Sr}_{0.12}\text{Cu}_{1-y}\text{Zn}_y\text{O}_4$ ($y = 0, 0.016$) [48]. The magnetic ordering wave vectors are $\mathbf{Q}_{\text{so}} = (0.5 - \delta, 0.5, 0)$ and $(0.5, 0.5 + \delta, 0)$, i.e., they are displaced by δ from the position of the magnetic Bragg peak in the AF parent compound La_2CuO_4 [5, 6]. In Fig. 4(a) we show h scans through the $(0.5 + \delta, 0.5, 0)$ magnetic superlattice peaks, recorded at $T = 1.75$ K for the samples $y = 0$ and 0.016 . It is clear that the intensity and incommensurability do not change with Zn doping. However, T_{so} is strongly suppressed from $T_{\text{so}} \simeq 50$ K [5] for $y = 0$ to $T_{\text{so}} \simeq 10$ K for $y = 0.016$, as demonstrated in Fig. 4(b), where the peak intensity is shown as a function of temperature.

Going further, we studied the Zn-impurity effects on T_{so} and T_c in $\text{La}_{1.845}\text{Ba}_{0.155}\text{CuO}_4$. This compound ($x > 1/8$) exhibits a well defined bulk SC transition with $T_c = 30$ K and at the same time shows static spin-stripe order $T_{\text{so}} \simeq T_c = 30$ K [24]. This enables us to study impurity effects on T_{so} and T_c simultaneously in the same sample. Figure 5a shows the temperature dependence of the magnetic volume fraction V_m extracted from ZF- μ SR data for $\text{La}_{1.845}\text{Ba}_{0.155}\text{Cu}_{1-y}\text{Zn}_y\text{O}_4$ ($y = 0, 0.02$, and 0.04). The low temperature value of V_m increases with increasing Zn content y and reaches 100 % for the highest Zn content $y = 0.04$. On the other hand, T_{so} decreases with increasing y similar as for 1/8-doping. The values of T_{so} and T_c (see the supplementary Note III and supplementary Figs. S2 and S3 [42]) as a function of Zn content y are shown in Fig. 5(b). Again, with increasing y both T_c and T_{so} decrease linearly with the same slope, indicating that Zn impurities influence T_c and T_{so} in the same manner.

What is the significance of this surprising correlation? Let us start with the fact that it is unusual to have spin order occur in a hole-doped cuprate at a temperature of ~ 35 K. Just a couple of percent of hole doping is generally sufficient to wipe out antiferromagnetic order [49].

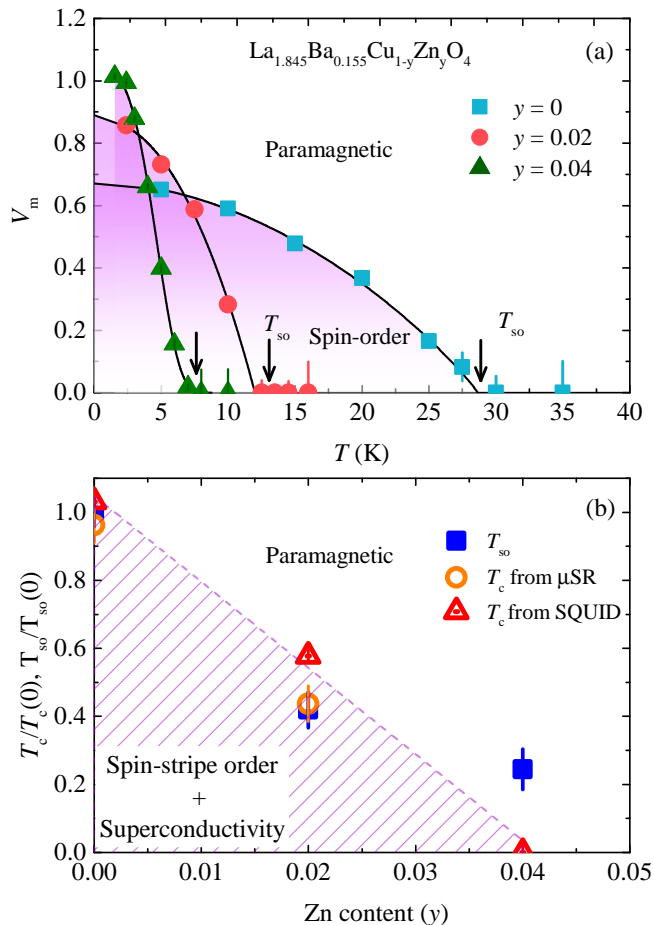


FIG. 5: (Color online) (a) Temperature dependence of the magnetic volume fraction V_m for $\text{La}_{1.845}\text{Ba}_{0.155}\text{Cu}_{1-y}\text{Zn}_y\text{O}_4$ ($y = 0, 0.02, 0.04$). (b) The normalized static spin-stripe order temperature $T_{so}/T_{so}(0)$ and the normalized superconducting transition temperature $T_c/T_c(0)$ for $\text{La}_{1.845}\text{Ba}_{0.155}\text{Cu}_{1-y}\text{Zn}_y\text{O}_4$ as a function of Zn content y . The dashed line is a guide to the eye.

One common point of view is that antiferromagnetism and superconductivity are competing orders [50]. From that perspective, one might take the occurrence of spin-stripe order as evidence that hole-pairing and superconductivity have been suppressed. In that case, we might expect the impact of Zn-doping on T_{so} to be similar to its impact on the Néel temperature in La_2CuO_4 . That assumption leads to a problem, however, as experiment has demonstrated that it takes, not 4%, but $\sim 40\%$ Zn to destroy Néel order [51]. One could also take account of the fact that the Zn tends to induce static Cu spin order in its immediate neighborhood [52, 53], which, with random locations of the Zn sites, could lead, at higher Zn concentrations, to some disorder from neighboring pinned stripe domains being out of phase with one another; however, a shortening of the spin correlation length only becomes apparent with at least 3% Zn doping [41, 54], while the drop in T_{so} is clear at much lower Zn concentrations.

Consider instead that previous experiments provide evidence that spin-stripe order coexists with two-dimensional superconducting correlations in LBCO-1/8 [19, 20]. Here, the superconducting and spin orders are intertwined [15]. Superconducting correlations within charge stripes must establish Josephson coupling across the spin stripes, while the spins in neighboring stripes must establish an effective exchange coupling via the fluctuating pairs in the intervening charge stripe. A Zn ion will locally suppress hole motion, thus eliminating local superconducting coherence and weakening the superconductivity [55]. Local suppression of hole hopping will also disrupt the effective exchange coupling between spin stripes, leading to a reduction in T_{so} .

Previous μSR studies of Zn doping in LSCO and $\text{YBa}_2\text{Cu}_3\text{O}_7$ have established the “Swiss-cheese” model: a fixed carrier density per Zn atom is removed from the superfluid density, as if each Zn removes a fixed areal fraction of the superfluid [56]. The linear relationship between T_c and the average superfluid density, valid for underdoped through optimally-doped cuprate HTSs, then explains the reduction of T_c with increasing Zn concentration [57]. For the stripe-ordered systems, it is plausible that both the superconducting and spin-stripe orders will respond in a similar fashion.

In conclusion, static spin-stripe order and superconductivity in cuprate systems $\text{La}_{2-x}\text{Ba}_x\text{Cu}_{1-y}\text{Zn}_y\text{O}_4$ ($x = 0.125, 0.155$) and $\text{La}_{1.48}\text{Nd}_{0.4}\text{Sr}_{0.12}\text{Cu}_{1-y}\text{Zn}_y\text{O}_4$ were studied by means of magnetisation, μSR , and neutron scattering experiments as a function of nonmagnetic Zn impurity concentration. High sensitivity of the static spin-stripe order temperature T_{so} to impurities in the CuO_2 plane was demonstrated. Namely, the spin-stripe ordering temperature T_{so} strongly decreases linearly with Zn doping and disappears at about 4% Zn content. More strikingly, T_{so} is suppressed in the same fashion as is the superconducting transition temperature T_c by Zn impurities. These results strongly suggest that the existence of the stripe order requires intertwining with the SC pairing correlations, such as occurs in the proposed PDW state. The present findings should help to better understand the complex interplay between stripe order and superconductivity in cuprates. More generally, since charge and spin orders are often observed in other transition-metal oxides, investigation of impurity effects and disorder on stripe formation may become an interesting research avenue in correlated electron systems.

Acknowledgments. The μSR experiments were carried out at the $\pi\text{M}3$ beam line of the Paul Scherrer Institute (Switzerland), using the general purpose instrument (GPS). The neutron scattering experiments were carried out with the three-axis spectrometer EIGER at the Swiss Spallation Neutron Source SINQ at the Paul Scherrer Institut (PSI), Switzerland. We are grateful to S.A. Kivelson for valuable discussions. Z.G. gratefully acknowledges the financial support by the Swiss

National Science Foundation (Early Postdoc Mobility SNF fellowship P2ZHP2-161980 and SNF Grant 200021-149486). Z.G. thanks Martin Mansson for useful discussions. A.S. acknowledges support from the SCOPES grant No. SCOPES IZ74Z0-160484. Work at Columbia University is supported by US NSF DMR-1436095 (DM-REF) and NSF DMR-1610633 as well as by REIMEI project of Japan Atomic Energy Agency. JMT is supported at Brookhaven by the U.S. Department of Energy, Office of Basic Energy Sciences, under contract No. DE-SC0012704.

* Electronic address: zg2268@columbia.edu

- [1] Bednorz, J.G., and Müller, K.A., *Z. Phys. B* **64**, 189 (1986).
- [2] Moodenbaugh, A.R., Xu, Y., Suenaga, M., Folkerts, T.J., and Shelton, R.N., Superconducting properties of $\text{La}_{2-x}\text{Ba}_x\text{CuO}_4$. *Phys. Rev. B* **38**, 4596 (1988).
- [3] Kivelson, S.A. *et al.* How to detect fluctuating stripes in the high-temperature superconductors. *Rev. Mod. Phys.* **75**, 1201 (2003).
- [4] Vojta, M. Lattice symmetry breaking in cuprate superconductors: Stripes, nematics, and superconductivity. *Adv. Phys.* **58**, 699 (2009).
- [5] Tranquada, J.M., Sternlieb, B.J., Axe, J.D., Nakamura, Y. and Uchida, S., Evidence for stripe correlations of spins and holes in copper oxide superconductors. *Nature (London)* **375**, 561 (1995).
- [6] Tranquada, J.M., Axe, J.D., Ichikawa, N., Nakamura, Y., Uchida, S. and Nachumi, B., Neutron-scattering study of stripe-phase order of holes and spins in $\text{La}_{1.48}\text{Nd}_{0.4}\text{Sr}_{0.12}\text{CuO}_4$. *Phys. Rev. B* **54**, 7489 (1996).
- [7] Abbamonte, P. *et al.* Spatially modulated 'Mottness' in $\text{La}_{2-x}\text{Ba}_x\text{CuO}_4$. *Nat. Phys.* **1**, 155 (2005).
- [8] Hücker, M. *et al.* Stripe order in superconducting $\text{La}_{2-x}\text{Ba}_x\text{CuO}_4$ ($0.095 \leq x \leq 0.155$). *Phys. Rev. B* **83**, 104506 (2011).
- [9] Luke, G.M. *et al.* Static Magnetic Order in $\text{La}_{1.875}\text{Ba}_{0.125}\text{CuO}_4$. *Physica C* **185-9**, 1175 (1991).
- [10] Guguchia, Z. *et al.* Negative Oxygen Isotope Effect on the Static Spin Stripe Order in Superconducting $\text{La}_{2-x}\text{Ba}_x\text{CuO}_4$ ($x = 1/8$) Observed by Muon-Spin Rotation. *Phys. Rev. Lett.* **113**, 057002 (2014).
- [11] M. Fujita *et al.*, "Stripe order, depinning, and fluctuations in $\text{La}_{1.875}\text{Ba}_{0.125}\text{CuO}_4$ and $\text{La}_{1.875}\text{Ba}_{0.075}\text{Sr}_{0.050}\text{CuO}_4$," *Phys. Rev. B* **70**, 104517 (2004).
- [12] Wu, T. *et al.* Magnetic-field-induced charge-stripe order in the high-temperature superconductor $\text{YBa}_2\text{Cu}_3\text{O}_y$. *Nature* **477**, 191-194 (2011).
- [13] Kohsaka, Y. *et al.* An Intrinsic Bond-Centered Electronic Glass with Unidirectional Domains in Underdoped Cuprates. *Science* **315**, 1380 (2007).
- [14] B. Keimer, S. A. Kivelson, M. R. Norman, S. Uchida, and J. Zaanen, "From quantum matter to high-temperature superconductivity in copper oxides," *Nature* **518**, 179 (2015).
- [15] Fradkin, E., Kivelson, S. A. and Tranquada, J. M. Colloquium: Theory of intertwined orders in high temperature superconductors. *Rev. Mod. Phys.* **87**, 457 (2015).
- [16] Himeda, A., Kato, T. and Ogata, M. Stripe States with Spatially Oscillating d -Wave Superconductivity in the Two-Dimensional t -J Model. *Phys. Rev. Lett.* **88**, 117001 (2002).
- [17] Berg, E. *et al.* Dynamical Layer Decoupling in a Stripe-Ordered High- T_c Superconductor. *Phys. Rev. Lett.* **99**, 127003 (2007).
- [18] Tranquada, J.M. Spins, stripes, and superconductivity in hole-doped cuprates. *AIP Conference Proceedings* **1550**, 114 (2013).
- [19] Tranquada, J.M. *et al.* Evidence for unusual superconducting correlations coexisting with stripe order in $\text{La}_{1.875}\text{Ba}_{0.125}\text{CuO}_4$. *Phys. Rev. B* **78**, 174529 (2008).
- [20] Li, Q. *et al.* Two-Dimensional Superconducting Fluctuations in Stripe-Ordered $\text{La}_{1.875}\text{Ba}_{0.125}\text{CuO}_4$. *Phys. Rev. Lett.* **99**, 067001 (2007).
- [21] Valla, T. *et al.* The Ground State of the Pseudogap in Cuprate Superconductors. *Science* **314**, 1914 (2006).
- [22] He, R.-H. *et al.* Energy gaps in the failed high- T_c superconductor $\text{La}_{1.875}\text{Ba}_{0.125}\text{CuO}_4$. *Nat. Phys.* **5**, 119-123 (2009).
- [23] J. F. Ding *et al.*, "Two-dimensional superconductivity in stripe-ordered $\text{La}_{1.6-x}\text{Nd}_{0.4}\text{Sr}_x\text{CuO}_4$ single crystals," *Phys. Rev. B* **77**, 214524 (2008).
- [24] Guguchia, Z. *et al.*, Cooperative coupling of static magnetism and bulk superconductivity in the stripe phase of $\text{La}_{2-x}\text{Ba}_x\text{CuO}_4$: Pressure ($x = 0.155, 0.17$) and doping ($x = 0.11-0.17$) dependent studies. *Phys. Rev. B* **94**, 214511 (2016).
- [25] Guguchia, Z. *et al.* Tuning the static spin-stripe phase and superconductivity in $\text{La}_{2-x}\text{Ba}_x\text{CuO}_4$ ($x = 1/8$) by hydrostatic pressure. *New J. Phys.* **15**, 093005 (2013).
- [26] Xu, Z. *et al.* Neutron-Scattering Evidence for a Periodically Modulated Superconducting Phase in the Underdoped Cuprate $\text{La}_{1.905}\text{Ba}_{0.095}\text{CuO}_4$. *Phys. Rev. Lett.* **113**, 177002 (2014).
- [27] Jacobsen, H. *et al.* Neutron scattering study of spin ordering and stripe pinning in superconducting $\text{La}_{1.93}\text{Sr}_{0.07}\text{CuO}_4$. *Phys. Rev. B* **92**, 174525 (2015).
- [28] Lee, P. A. Amperean Pairing and the Pseudogap Phase of Cuprate Superconductors. *Phys. Rev. X* **4**, 031017 (2014).
- [29] Yu, F. *et al.* Magnetic phase diagram of underdoped $\text{YBa}_2\text{Cu}_3\text{O}_y$ inferred from torque magnetization and thermal conductivity. *Proc. Natl. Acad. Sci.* **113**, 12667 (2016).
- [30] Xiao, G., Cieplak, M.Z., Xiao, J.Q., and Chien, C.L., Magnetic pair-breaking effects: Moment formation and critical doping level in superconducting $\text{La}_{1.85}\text{Sr}_{0.15}\text{Cu}_{1-x}\text{A}_x\text{O}_4$ systems ($A = \text{Fe, Co, Ni, Zn, Ga, Al}$). *Phys. Rev. B* **42**, 8752 (1990).
- [31] Y. Fukuzumi, K. Mizuhashi, K. Takenaka, and S. Uchida. Universal Superconductor-Insulator Transition and T_c Depression in Zn-Substituted High/ T_c Cuprates in the Underdoped Regime. *Phys. Rev. Lett.* **76**, 684 (1996).
- [32] S. Komiya and Y. Ando, Electron localization in $\text{La}_{2-x}\text{Sr}_x\text{CuO}_4$ and the role of stripes. *Phys. Rev. B* **70**, 060503(R) (2004).
- [33] P. Mendels *et al.*, "Muon-spin-rotation study of the effect of Zn substitution on magnetism in $\text{YBa}_2\text{Cu}_3\text{O}_x$," *Phys. Rev. B* **49**, 10035 (1994).
- [34] Akoshima, M., Koike, Y., Watanabe, I., Nagamine, K., Anomalous muon-spin relaxation in the Zn-substituted

- YBa₂Cu_{3-2y}Zn_{2y}O_{6+δ} around the hole concentration of $\frac{1}{8}$ per Cu. *Phys. Rev. B* **62**, 6761 (2000).
- [35] Watanabe, I., Akoshima, M., Koike, Y., Ohira, S., Nagamine, K., Muon-spin-relaxation study on the Cu-spin state of Bi₂Sr₂Ca_{1-x}Y_x(Cu_{1-y}Zn_y)₂O_{8+δ} around the hole concentration of $\frac{1}{8}$ per Cu. *Phys. Rev. B* **62**, 14524 (2000).
- [36] Adachi, T., Yairi, S., Koike, Y., Watanabe, I., Nagamine, K., Muon-spin-relaxation and magnetic-susceptibility studies of the effects of the magnetic impurity Ni on the Cu-spin dynamics and superconductivity in La_{2-x}Sr_xCu_{1-y}Ni_yO₄ with $x = 0.13$. *Phys. Rev. B* **70**, 060504(R) (2004).
- [37] T. Adachi, S. Yairi, K. Takahashi, Y. Koike, I. Watanabe, K. Nagamine, Muon spin relaxation and magnetic susceptibility studies of the effects of nonmagnetic impurities on the Cu spin dynamics and superconductivity in La_{2-x}Sr_xCu_{1-y}Zn_yO₄ around $x = 0.115$. *Phys. Rev. B* **69**, 184507 (2004).
- [38] Koike, Y., and Adachi, T., Impurity and magnetic field effects on the stripes in cuprates. *Physica C* **481**, 115 (2012).
- [39] O. Anegawa, Y. Okajima, S. Tanda, and K. Yamaya, Effect of spin substitution on stripe order in La_{1.875}Ba_{0.125}Cu_{1-y}M_yO₄ ($M = \text{Zn}$ or Ni). *Phys. Rev. B* **63**, 140506 (2001).
- [40] J. Takeda, T. Inukai, and M. Sato, Electronic specific heat of (La,Nd)_{2-x}Sr_xCu_{1-y}Zn_yO₄ up to about 300 K. *Journal of Physics and Chemistry of Solids* **62**, 181 (2001).
- [41] Fujita, M. *et al.* Neutron-Scattering Study of Impurity Effect on Stripe Correlations in La-Based 214 High- T_c Cuprate. *J. Supercond. Nov. Magn.* **22**, 243 (2009).
- [42] See Supplemental Material at [URL will be inserted by publisher] for details on the μSR technique and analysis, and further experimental characterizations of the samples, which includes Refs. [1–4]
- [43] U. Stuhr, B. Roessli, S. Gvasaliya, H.M. Rønnow, U. Filges, D. Graf, A. Bollhalder, D. Hohl, R. Bürge, M. Schild, L. Holitzner, C. Kaegi, P. Keller and T. Mühlbach. The thermal triple-axis-spectrometer EIGER at the continuous spallation source SINQ. *Nucl. Instrum. Methods Phys. Res., Sect. A* **853**, 16 (2017).
- [44] Nachumi, B. *et al.* Muon spin relaxation study of the stripe phase order in La_{1.6-x}Nd_{0.4}Sr_xCuO₄ and related 214 cuprates. *Phys. Rev. B* **58**, 8760-8772 (1998).
- [45] J. Arai, T. Ishiguro, T. Goko, S. Iigaya, K. Nishiyama, I. Watanabe, and K. Nagamine, *Journal of Low Temperature Physics* **131**, 375 (2003).
- [46] Suter, A. and Wojek, B.M. Musrfit: a free platform-independent framework for μSR data analysis. *Physics Procedia* **30**, 69-73 (2012).
- [47] M.K. Crawford, R.L. Harlow, E.M. McCarron, W.E. Farneth, J.D. Axe, H. Chou, and Q. Huang, Lattice instabilities and the effect of copper-oxygen-sheet distortions on superconductivity in doped La₂CuO₄. *Phys. Rev. B* **44**, 749 (1991).
- [48] Note that this is the nominal composition of the crystals, based on the starting materials; the actual composition could differ slightly from that of the polycrystalline samples discussed earlier.
- [49] M. Matsuda, M. Fujita, K. Yamada, R. J. Birgeneau, Y. Endoh, and G. Shirane, “Electronic phase separation in lightly-doped La_{2-x}Sr_xCuO₄,” *Phys. Rev. B* **65**, 134515 (2002).
- [50] S. Sachdev, “Quantum Criticality: Competing Ground States in Low Dimensions,” *Science* **288**, 475 (2000).
- [51] O. P. Vajk, P. K. Mang, M. Greven, P. M. Gehring, and J. W. Lynn, “Quantum Impurities in the Two-Dimensional Spin One-Half Heisenberg Antiferromagnet,” *Science* **295**, 1691 (2002).
- [52] A. V. Mahajan, H. Alloul, G. Collin, and J. F. Marucco, “⁸⁹Y NMR Probe of Zn Induced Local Moments in YBa₂(Cu_{1-y}Zn_y)₃O_{6+x},” *Phys. Rev. Lett.* **72**, 3100 (1994).
- [53] M.-H. Julien *et al.*, “⁶³Cu NMR Evidence for Enhanced Antiferromagnetic Correlations around Zn Impurities in YBa₂Cu₃O_{6.7},” *Phys. Rev. Lett.* **84**, 3422 (2000).
- [54] H. Kimura, K. Hirota, H. Matsushita, K. Yamada, Y. Endoh, S.-H. Lee, C.F. Majkrzak, R. Erwin, G. Shirane, M. Greven, Y.S. Lee, M.A. Kastner, and R.J. Birgeneau, Neutron-scattering study of static antiferromagnetic correlations in La_{2-x}Sr_xCu_{1-y}Zn_yO₄. *Phys. Rev. B* **59**, 6517 (1999).
- [55] C.M. Smith, A.H. Castro Neto, and A.V. Balatsky, T_c suppression in co-doped striped cuprates. *Phys. Rev. Lett.* **87**, 177010 (2001).
- [56] Nachumi, B. *et al.* Muon Spin Relaxation Studies of Zn-Substitution Effects in High- T_c Cuprate Superconductors. *Phys. Rev. Lett.* **77**, 5421 (1996).
- [57] Y. J. Uemura *et al.* Universal Correlations between T_c and n_s/m^* (Carrier Density over Effective Mass) in High- T_c cuprate superconductors. *Phys. Rev. Lett.* **62**, 2317 (1989).

SUPPLEMENTAL MATERIAL

METHODS

Sample preparation: Polycrystalline samples of $\text{La}_{1.875}\text{Ba}_{0.125}\text{Cu}_{1-y}\text{Zn}_y\text{O}_4$ with $y = 0, 0.02, 0.04$ and $\text{La}_{1.48}\text{Nd}_{0.4}\text{Sr}_{0.12}\text{Cu}_{1-y}\text{Zn}_y\text{O}_4$ with $y = 0, 0.01, 0.02, 0.04$ were prepared by the conventional solid-state reaction method using La_2O_3 , Nd_2O_3 , BaCO_3 , SrCO_3 , and CuO . The single-phase character of the samples was checked by powder x-ray diffraction. The single crystals of $\text{La}_{1.48}\text{Nd}_{0.4}\text{Sr}_{0.12}\text{Cu}_{1-y}\text{Zn}_y\text{O}_4$ ($y = 0, 0.016$) were grown by the traveling solvent floating zone method. All the measurements were performed on samples from the same batch.

Principles of the μSR technique: Static spin-stripe orders in $\text{La}_{1.875}\text{Ba}_{0.125}\text{Cu}_{1-y}\text{Zn}_y\text{O}_4$ with $y = 0, 0.02, 0.04$ and $\text{La}_{1.48}\text{Nd}_{0.4}\text{Sr}_{0.12}\text{Cu}_{1-y}\text{Zn}_y\text{O}_4$ with $y = 0, 0.01, 0.02, 0.04$ were studied by means of zero-field (ZF) μSR experiments. The μSR experiments were carried out at the πM3 beam line of the Paul Scherrer Institute (Switzerland), using the general purpose instrument (GPS). In a μSR experiments an intense beam ($p_\mu = 29 \text{ MeV}/c$) of 100 % spin-polarized muons is stopped in the sample mounted

inside of a gas-flow ^4He cryostat on a sample holder with a standard veto setup providing essentially a background free μSR signal. The positively charged muons thermalize in the sample at interstitial lattice sites, where they act as magnetic microprobes. In a magnetic material the muons spin precess in the local field B_μ at the muon site with the Larmor frequency $\nu_\mu = \gamma_\mu/(2\pi)B_\mu$ (muon gyromagnetic ratio $\gamma_\mu/(2\pi) = 135.5 \text{ MHz T}^{-1}$). In a ZF μSR experiment positive muons implanted into a sample serve as an extremely sensitive local probe to detect small internal magnetic fields and ordered magnetic volume fractions in the bulk of magnetic materials. Thus, μSR is a particularly powerful tool to study inhomogeneous magnetism in materials.

The muons μ^+ implanted into the sample will decay after a mean life time of $\tau_\mu = 2.2 \mu\text{s}$, emitting a fast positron e^+ preferentially along their spin direction. Various detectors placed around the sample track the incoming μ^+ and the outgoing e^+ . When the muon detector records the arrival of a μ in the specimen, the electronic clock starts. The clock is stopped when the decay positron e^+ is registered in one of the e^+ detectors, and the measured time interval is stored in a histogramming memory. In this way a positron-count versus time histogram is formed. A muon decay event requires that within a certain time interval after a μ^+ has stopped in the sample a e^+ is detected. This time interval extends usually over several muon lifetimes (e.g. $10\mu\text{s}$). After a bunch of muons stopped in the sample, one obtains a histogram for the forward (N_{e^+F}) and the backward (N_{e^+B}) detectors, which in the ideal case has the following form:

$$N_{e^+\alpha}(t) = N_0 e^{-\frac{t}{\tau_\mu}} (1 + A_0 \vec{P}(t) \hat{n}_\alpha) + N_{bgr}. \quad \alpha = F, B \quad (1)$$

Here, the exponential factor accounts for the radioactive muon decay. $\vec{P}(t)$ is the muon-spin polarization function with the unit vector \hat{n}_α ($\alpha = F, B$) with respect to the incoming muon spin polarization. N_0 is number of positrons at the initial time $t=0$. N_{bgr} is a background contribution due to uncorrelated starts and stops. A_0 is the initial asymmetry, depending on different experimental factors, such as the detector solid angle, efficiency, absorption, and scattering of positrons in the material. Typical values of A_0 are between 0.2 and 0.3.

Since the positrons are emitted predominantly in the direction of the muon spin which precesses with ω_μ , the forward and backward detectors will detect a signal oscillating with the same frequency. In order to remove the exponential decay due to the finite life time of the muon, the so-called asymmetry signal $A(t)$ is calculated:

$$A(t) = \frac{N_{e^+F}(t) - N_{e^+B}(t)}{N_{e^+F}(t) + N_{e^+B}(t)} = A_0 P(t), \quad (2)$$

where, $N_{e^+F}(t)$ and $N_{e^+B}(t)$ are the number of positrons detected in the forward and backward detectors, respectively. The quantities $A(t)$ and $P(t)$ depend sensitively on the spatial distribution and dynamical fluctuations of the magnetic environment of the muons. Hence, these functions allow to study interesting physics of the investigated system.

Analysis of ZF- μSR data:

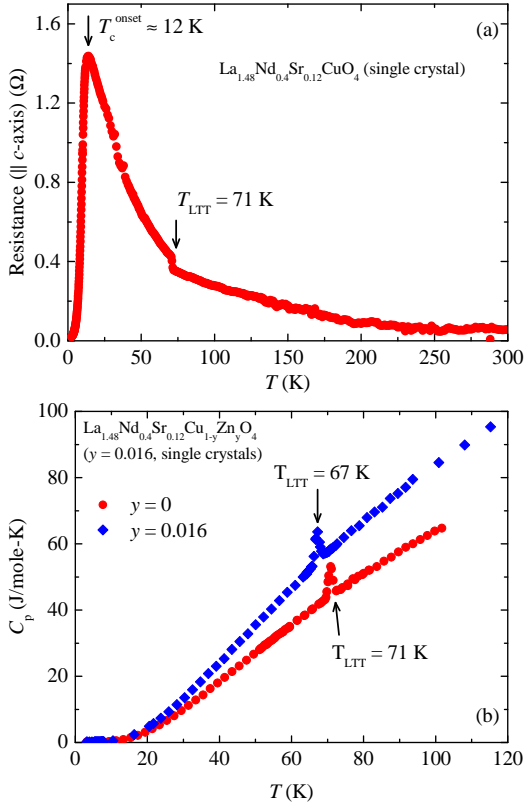


FIG. 6: (Color online) (a) Temperature dependence of the resistance along the c -axis for the single crystal of $\text{La}_{1.48}\text{Nd}_{0.4}\text{Sr}_{0.12}\text{CuO}_4$. (b) The specific heat C_p as a function of temperature for the single crystals of $\text{La}_{1.48}\text{Nd}_{0.4}\text{Sr}_{0.12}\text{Cu}_{1-y}\text{Zn}_y\text{O}_4$ ($y = 0, 0.016$). The arrows denote the LTT structural phase transition temperatures T_{LTT} .

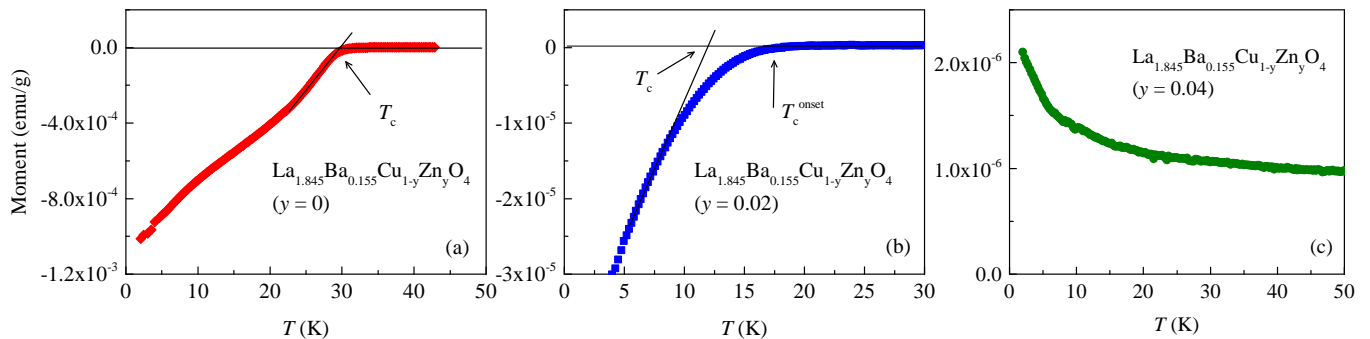


FIG. 7: (Color online) Temperature dependence of the diamagnetic moment of $\text{La}_{1.845}\text{Ba}_{0.155}\text{Cu}_{1-y}\text{Zn}_y\text{O}_4$ for various $y = 0, 0.02$ and 0.04 , measured in a magnetic field of $\mu_0 H = 0.5$ mT. The arrows denote the superconducting transition temperature T_c .

The μSR signals in the whole temperature range were analyzed by decomposing the signal into a magnetic and a nonmagnetic contribution:

$$P(t) = V_m \left[\frac{2}{3} e^{-\lambda_T t} J_0(\gamma_\mu B_\mu t) + \frac{1}{3} e^{-\lambda_L t} \right] + (1 - V_m) e^{-\lambda_{nm} t}. \quad (3)$$

Here, V_m denotes the relative volume of the magnetic fraction, and B_μ is the average internal magnetic field at the muon site. λ_T and λ_L are the depolarization rates representing the transversal and the longitudinal relaxing components of the magnetic parts of the sample. J_0 is the zeroth-order Bessel function of the first kind. This is characteristic for an incommensurate spin density wave and has been observed in cuprates with static spin stripe order [1]. λ_{nm} is the relaxation rate of the nonmagnetic part of the sample, where spin-stripe order is absent. The μSR time spectra were analyzed using the free software package MUSRFIT [2].

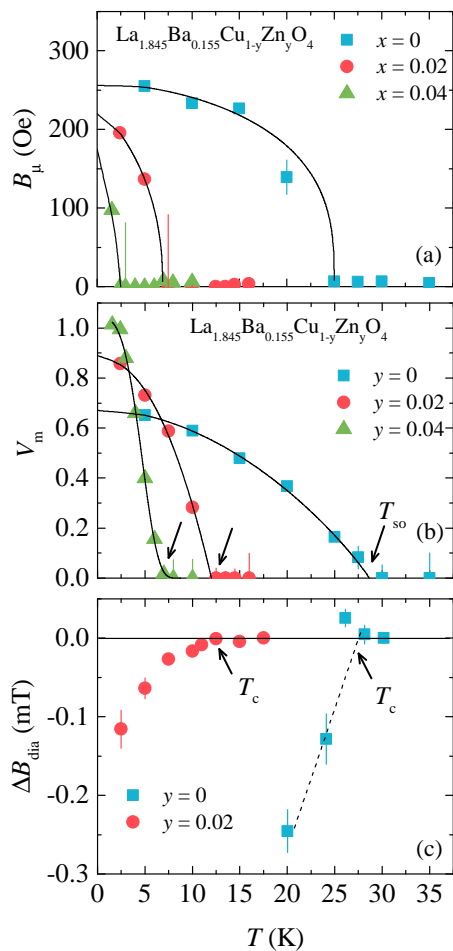


FIG. 8: (Color online) Temperature dependence of the internal magnetic field B_μ (a) and magnetic volume fraction V_m (b) in $\text{La}_{1.845}\text{Ba}_{0.155}\text{Cu}_{1-y}\text{Zn}_y\text{O}_4$ ($y = 0, 0.02, 0.04$). The solid lines are fits of the data to the same empirical power law as described in the manuscript. (c) Diamagnetic shift ΔB_{dia} of $\text{La}_{1.845}\text{Ba}_{0.155}\text{Cu}_{1-y}\text{Zn}_y\text{O}_4$ ($y = 0, 0.02, 0.04$) as a function of temperature. The arrows denote T_c .

STUDIES OF TRANSPORT, THERMODYNAMIC AND STRUCTURAL PROPERTIES

Figure 6a shows the temperature dependence of the c -axis resistance for the single crystal of $\text{La}_{1.48}\text{Nd}_{0.4}\text{Sr}_{0.12}\text{CuO}_4$. A clear jump in resistance (R) appears at $T_{\text{LTT}} \simeq 71$ K, which is indicated by an arrow and ascribed to the structural phase transition from low-temperature orthorhombic (LTO) to low-temperature tetragonal (LTT) phase. Upon lowering the temperature below $T_{\text{LTT}} \simeq 71$ K, R monotonically increases down to 12 K, below which it decreases and reaches zero resistance state towards the base temperature. This indicates that while the onset of SC transition is at T_{SC} in $\text{La}_{1.48}\text{Nd}_{0.4}\text{Sr}_{0.12}\text{CuO}_4$ is at $\simeq 12$ K, bulk superconductivity is only reached at the base temperature $T_c \simeq 2$ K.

Figure 6b shows the specific heat C_p as a function of temperature for the single crystals of $\text{La}_{1.48}\text{Nd}_{0.4}\text{Sr}_{0.12}\text{Cu}_{1-y}\text{Zn}_y\text{O}_4$ ($y = 0, 0.016$). Clear peak [3, 4] in C_p at $T_{\text{LTT}} \simeq 71$ K is observed for $y = 0$ sample, which is in perfect agreement with the resistance data. In Zn-doped sample $y = 0.016$ the peak appears at slightly lower temperature $T_{\text{LTT}} \simeq 67$ K, indicating very tiny impact of the Zn-doping on the bulk LTT structural phase transition temperature.

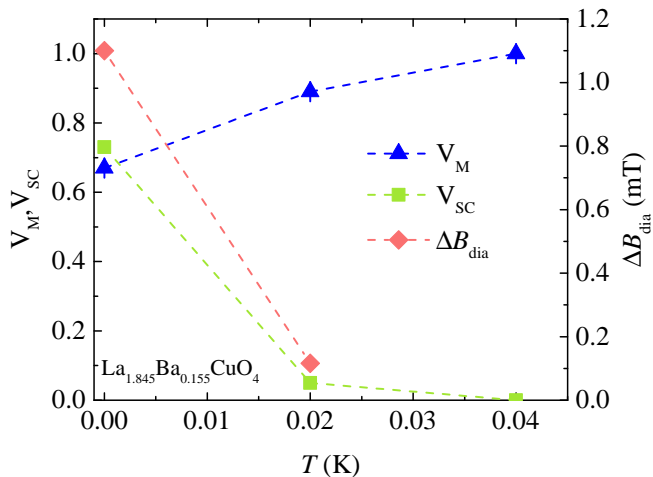


FIG. 9: (Color online) The base temperature values of magnetic volume fraction V_m , the superconducting volume fraction V_{SC} and the diamagnetic shift ΔB_{dia} for $\text{La}_{1.845}\text{Ba}_{0.155}\text{Cu}_{1-y}\text{Zn}_y\text{O}_4$ as a function of Zn-doping. The dashed lines are a guide to the eyes.

SUPERCONDUCTING PROPERTIES OF $\text{La}_{1.845}\text{Ba}_{0.155}\text{Cu}_{1-y}\text{Zn}_y\text{O}_4$, STUDIED BY MEANS OF MAGNETIZATION AND MUON-SPIN ROTATION EXPERIMENTS

Figure 7 shows the temperature dependence of the zero-field-cooled (ZFC) diamagnetic moment m_{ZFC} for $\text{La}_{1.845}\text{Ba}_{0.155}\text{Cu}_{1-y}\text{Zn}_y\text{O}_4$ ($y = 0, 0.02, 0.04$) sample, recorded in a magnetic field of $\mu_0 H = 0.5$ mT. The diamagnetic moment as well as T_c are strongly suppressed by Zn-substitution.

Figures 8a and b show the temperature dependence of the internal magnetic field B_μ and the magnetic volume fraction V_m extracted from the ZF- μ SR data for $\text{La}_{1.845}\text{Ba}_{0.155}\text{Cu}_{1-y}\text{Zn}_y\text{O}_4$ ($y = 0, 0.02$ and 0.04). The low temperature value of V_m increases with increasing Zn-content y . Note that $V_m = 100\%$ for $y = 0.04$. On the other hand, the static spin-stripe order temperature T_{so} decreases with increasing y as it is the case for T_c .

The SC response of the samples was also measured by using TF- μ SR. For all the samples a diamagnetic shift of $\mu_0 H_{int}$ experienced by the muons is observed below T_c . This is evident in Fig. 8c where we plot the temperature dependence of the diamagnetic shift $\Delta B_{dia} = \mu_0 [H_{int,SC} - H_{int,NS}]$ for $\text{La}_{1.845}\text{Ba}_{0.155}\text{Cu}_{1-y}\text{Zn}_y\text{O}_4$ ($y = 0, 0.02$ and

0.04), where $\mu_0 H_{int,SC}$ denotes the internal field measured in the SC state and $\mu_0 H_{int,NS}$ is the internal field measured in the normal state. Note that $\mu_0 H_{int,NS}$ is temperature independent. The SC transition temperature T_c is determined from the intercept of the linearly extrapolated ΔB_{dia} curve and its zero line. The diamagnetic shift ΔB_{dia} decreases strongly with increasing Zn-content y , which is consistent with the reduction of the diamagnetic moment as a result of Zn-substitution. In Fig. 8b of the main text, the values of T_c and T_{so} are plotted as a function of Zn-content y . Remarkably, both T_c and T_{so} decrease linearly with increasing y , indicating that Zn impurities influence T_c and T_{so} in the same way. These experiments give strong support to our high pressure data, showing the simultaneous occurrence of static magnetism and superconductivity in the LBCO-0.155 system.

Figure 9 shows the Zn-doping evolution of the base temperature values of the magnetic volume fraction, the superconducting volume fraction (estimated from the susceptibility data) and the diamagnetic shift, imposed by the SC state (extracted from μ SR). It is clear that while the magnetic fraction is enhanced by Zn-doping, the SC fraction is reduced substantially. Since already for 2 %-doped sample the SC fraction is small, it is impossible to extract the reliable information about the superfluid density. Only parameters we can get is the critical temperature and the strength of the diamagnetism.

* Electronic address: zg2268@columbia.edu

- [1] Nachumi, B. *et al.* Muon spin relaxation study of the stripe phase order in $\text{La}_{1.6-x}\text{Nd}_{0.4}\text{Sr}_x\text{CuO}_4$ and related 214 cuprates. *Phys. Rev. B* **58**, 8760-8772 (1998).
- [2] Suter, A. and Wojek, B.M. Musrfit: a free platform-independent framework for μ SR data analysis. *Physics Procedia* **30**, 69-73 (2012).
- [3] J. Takeda, T. Inukai, and M. Sato, Electronic specific heat of $(\text{La,Nd})_{2-x}\text{Sr}_x\text{Cu}_{1-y}\text{Zn}_y\text{O}_4$ up to about 300 K. *Journal of Physics and Chemistry of Solids* **62**, 181 (2001).
- [4] M.K. Crawford, R.L. Harlow, E.M. McCarron, W.E. Farneth, J.D. Axe, H. Chou, and Q. Huang, Lattice instabilities and the effect of copper-oxygen-sheet distortions on superconductivity in doped La_2CuO_4 . *Phys. Rev. B* **44**, 749 (1991).